DALTON
FULL PAPER

Structural and photomagnetic studies of a 1-D bimetallic chain $[Mn^{II}_2(L)_2(H_2O)][Mo^{IV}(CN)_8]\cdot 5H_2O$ (L = macrocycle): analogy with the photo-oxidation of $K_4[Mo^{IV}(CN)_8]\cdot 2H_2O$

Guillaume Rombaut,*[a] Stéphane Golhen,[b] Lahcène Ouahab,[b] Corine Mathonière[a] and (the late) Olivier Kahn[a]

[a] *Laboratoire des Sciences Moléculaires, Institut de Chimie de la Matière Condensée de Bordeaux, UPR CNRS No. 9048, F-33608 Pessac, France. E-mail: rombaut@icmcb.u-bordeaux.fr*

[b] *Laboratoire de Chimie du Solide et Inorganique Moléculaire, Université de Rennes I, UMR CNRS No. 6511, F-35042 Rennes, France*

Received 18th May 2000, Accepted 21st August 2000
First published as an Advance Article on the web 19th September 2000

A one-dimensional chain $[Mn^{II}_2(L)_2(H_2O)][Mo^{IV}(CN)_8]\cdot 5H_2O$ **2** (L = 2,13-dimethyl-3,6,9,12,18-pentaazabicyclo-[12.3.1]octadeca-1(18),2,12,14,16-pentaene, macrocyclic ligand) has been prepared from the reaction of $K_4[Mo^{IV}(CN)_8]\cdot 2H_2O$ **1** with the complex $[Mn^{II}L(H_2O)_2]Cl_2\cdot 4H_2O$ and its structure and photomagnetic properties have been studied. The structure of **2** consists of a polymeric zigzag chain of alternating Mn(L) and $Mo(CN)_8$ units with another Mn(L) unit linked to the Mo as a pendant arm. The paramagnetic compound **2** shows important modifications of its magnetic properties under UV-light irradiation, leading to the formation of ferrimagnetic chains. This non-reversible photomagnetic effect is thought to be caused by an internal photo-oxidation of Mo^{IV} (diamagnetic) to Mo^{V} (paramagnetic) as observed in the precursor **1**. The crystallographic data seem to indicate that the formation of hydrogen bonds between water molecules and nitrogen atoms of non-bridging cyano groups is a key factor to observe the molybdenum photo-oxidation.

Introduction

The control of magnetic properties by an external stimulus is one of the main challenges in the field of molecular sciences. In 1996, Sato *et al.* reported, for the first time, the observation of photo-induced magnetisation at low temperature in a Prussian blue analogue $K_{0.2}Co_{1.4}[Fe(CN)_6]\cdot 6.9H_2O$.[1,2] This phenomenon, leading to an increase of the Curie temperature from 16 to 19 K, is thermally or light reversible and thought to be caused by an internal photochemical redox reaction between the cobalt and iron sites. Up to now, all the results in the field of photomagnetism on metal-based molecular systems have concerned hexacyanometalates,[3–7] iron(II) spin-crossover compounds showing Light Induced Spin State Trapping (LIESST) effect[8–10] or metallo-organic compounds.[11,12] In the latter case the photomagnetic property is induced by the photochemical generation of triplet carbene centers from diazo groups creating new magnetic interactions with the metal centers.

We decided to work on the octacyanometalate precursors $[M(CN)_8]^{n-}$ (M = Mo or W) which are attractive for two main reasons. First, in this molecular geometry, the metal ion can be in two stable oxidation states: M^{IV} (diamagnetic, $S = 0$) or M^{V} (paramagnetic, $S = 1/2$). Secondly, the solution photochemistry of these precursors has been known for a long time. Indeed, on the one hand, the light irradiation of a solution containing $[M^{IV}(CN)_8]^{4-}$ in the charge transfer bands results in photo-oxidation of M^{IV} to M^{V} with ejection of a solvated electron.[13–18] On the other hand, if an aqueous solution of the precursor is irradiated in the range of the ligand field bands it mainly leads to photo-aquation products.[19–22]

Recently, we synthesized compounds with these $[M(CN)_8]^{n-}$ as building blocks. By using 3d metallic ions in the 2+ oxidation state (Fe^{II}, Mn^{II}, Cu^{II} ...), systems of general formula $[M^{II}(H_2O)_2]_2[M^{IV}(CN)_8]\cdot xH_2O$ were obtained but not structurally and magnetically characterised.[23] The crystal structure of the iron(II) phase has been solved and found to form a three-dimensional alternate array of $Fe(H_2O)_2^{2+}$ and $Mo^{IV}(CN)_8^{4-}$ units. This compound presents weak antiferromagnetic interactions at low temperature.[24] The copper(II) compound shows particular reversible modifications of its magnetic properties under light irradiation, confirming the intervalence charge transfer behaviour observed in solution.[25,26]

When metal complexes containing polydentate ligands (blocking some co-ordination sites) are used instead of simple aqua complexes, a great variety of cyanide-bridged bimetallic systems can be obtained.[27–32] This chemical route has been employed successfully in hexacyano- and heptacyano-metalate chemistry,[33] leading in the case of cyanomolybdate to a particular mixed valence Mo^{III}–Mo^{IV} three-dimensional compound with a heart shape structure.[34] This system has been synthesized from a transition metal complex with two available co-ordination sites in axial position of the type $Mn^{II}(L)$ (L = 2,13-dimethyl-3,6,9,12,18-pentaazabicyclo[12.3.1]octadeca-1(18),2,12,14,16-pentaene, macrocyclic ligand).

We report here, as a part of our work on the photomagnetic properties of molecular compounds, the synthesis and structure of a new 1-D bimetallic chain formulated as $[Mn^{II}_2(L)_2(H_2O)][Mo^{IV}(CN)_8]\cdot 5H_2O$ **2** using the octacyanometalate building block $K_4[Mo^{IV}(CN)_8]\cdot 2H_2O$ **1**. The photomagnetic properties of **1** and **2** have been studied under UV-light irradiation at low temperature. The results obtained on both compounds will be discussed on the basis of crystallographic data.

Experimental

Synthesis

Details of the preparation of $K_4[Mo^{IV}(CN)_8]\cdot 2H_2O$ **1** are given

DOI: 10.1039/b003983g

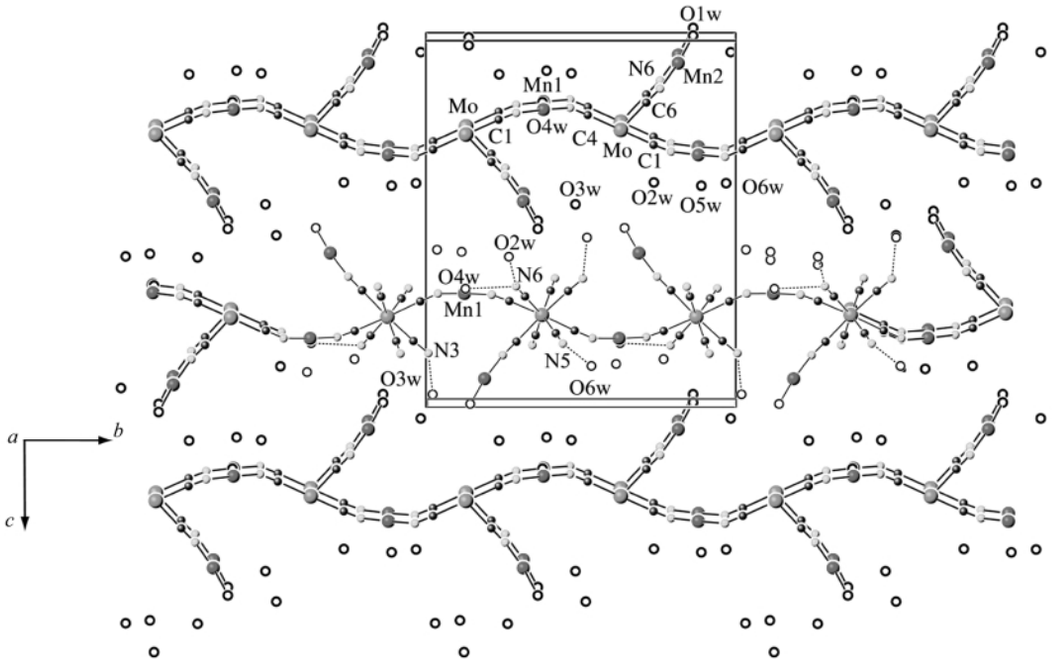

Fig. 1 A perspective view of chains along the *b* axis for complex **2**. Hydrogen atoms and the macrocycle around the manganese atoms are omitted for clarity.

elsewhere.[35] The manganese complex $[MnL(H_2O)_2]Cl_2{\cdot}4H_2O$ was synthesized according to the procedure described.[36]

$[Mn^{II}_2(L)_2(H_2O)][Mo^{IV}(CN)_8]{\cdot}5H_2O$ 2. Orange single crystals suitable for X-ray analysis were obtained by slow diffusion in an H-shaped tube of two aqueous solutions containing $K_4[Mo^{IV}(CN)_8]{\cdot}2H_2O$ (10^{-3} M) and $[MnL(H_2O)_2]Cl_2{\cdot}4H_2O$ (2×10^{-3} M), respectively.

Crystallographic data collection and structure determination

A single crystal of complex **2** was mounted on a Nonius Kappa CCD area-detector diffractometer equipped with a graphite monochromated Mo-Kα radiation source ($\lambda = 0.71073$ Å) and crystal data were collected at room temperature. For data reduction and cell refinement the programs DENZO and SCALEPACK were applied.[37] The structure was solved by direct methods with SHELXS 97,[38] and refined with SHELXL 97[38] programs by full-matrix least squares on F^2. The crystal data are summarised in Table 1. All non-hydrogen atoms were refined anisotropically. An isotropic thermal parameter 1.2 or 1.5 times that of the parent atom was assigned to hydrogen atoms which were allowed to ride.

CCDC reference number 186/2151.

See http://www.rsc.org/suppdata/dt/b0/b003983g/ for crystallographic files in .cif format.

Physical measurements

The infrared (IR) spectra were recorded on a Perkin-Elmer FT-IR Paragon 1000 spectrometer using KBr pellets. The optical experiments were performed on a Cary 5E spectrophotometer equipped with a diffusion sphere. ESR spectra were collected on a Bruker EMX spectrometer operating in the X band (9.46 GHz) equipped with an Oxford ESR-900 flowing-helium cryostat (4.2–300 K) controlled by an Oxford ITC4 temperature control unit.

The magnetic measurements were carried out with a Quantum Design MPMS-5S SQUID magnetometer working in dc mode down to 2 K and up to 50 kOe. The diamagnetic corrections for the compounds were estimated using Pascal's constants, and magnetic data were corrected for diamagnetic contributions of the sample holder.

Photomagnetic experiments were performed using a Kr^+ laser coupled through an optical fiber to the SQUID magnetometer cavity. Each sample consisted of a very thin layer of crystalline compound supported by a diamagnetic holder. Irradiation of both complexes **1** and **2** was carried out using a multi-line at 337 and 356 nm under a magnetic field of 10 kOe at 10 K. The output power of the panel meter was adjusted to 15 mW cm^{-2}. Magnetic properties were recorded before and after irradiation, in each case the light being turned off to avoid thermal inhomogeneities.

Results and discussion

The complex $[MnL(H_2O)_2]Cl_2{\cdot}4H_2O$ reacts with $K_4[Mo^{IV}(CN)_8]{\cdot}2H_2O$ to yield the 1-D cyanide-bridged compound $[Mn^{II}_2(L)_2(H_2O)][Mo^{IV}(CN)_8]{\cdot}5H_2O$ in aqueous solution. The IR spectrum exhibits some bands due to the presence of the macrocycle L (NH stretching vibration at 3221 cm^{-1} and C=N stretching vibration at 1648 cm^{-1} in particular) and two broad bands at 2121 and 2103 cm^{-1} which are assigned to CN stretching vibrations of bridging and terminal cyano groups, respectively. Compound **2** shows absorption bands in the UV-visible range which correspond to the sum of the $[MnL(H_2O)_2]Cl_2{\cdot}4H_2O$ and $K_4[Mo^{IV}(CN)_8]{\cdot}2H_2O$ bands.[39]

Crystal structure of $[Mn^{II}_2(L)_2(H_2O)][Mo^{IV}(CN)_8]{\cdot}5H_2O$ 2

The structure contains three metal sites localised on a general position, one molybdenum site and two manganese sites. The organisation is one dimensional and it is made up of chains running in a zigzag fashion along the *b* direction. Each chain consists of alternate Mn1(L) and Mo1$(CN)_8$ units, the Mn2(L) unit being linked to the Mo1 one as a pendant arm, as shown in Fig. 1.

The molybdenum atom is surrounded by eight cyano groups with a co-ordination reminiscent of a square antiprism. The first square N1–N2–N3–N7 is lightly distorted (N···N distances in the range 3.895(6)–4.080(7) Å, with angles in the range 86.05(13)–94.1(2)°). It forms an angle of 1.59(6)° with the second N4–N5–N6–N8 distorted square (N···N distances ranging from 3.893(6) to 4.079(6) Å, with angles in the range 87.30(11)–92.47(11)°). These two squares are twisted, the mean dihedral angle between two edges from the two squares being 44.8°. Two cyano groups are linked to two Mn1 sites yielding the Mn1–N4–C4–Mo–C1–N1–Mn1 infinite chain in

Table 1 Crystal data and structure refinement for complex **2**

Chemical formula	$C_{38}H_{54}Mn_2MoN_{18}O_6$
Formula weight	1064.81
Crystal system	Monoclinic
Space group	$P2_1/c$
a/Å	13.2063(4)
b/Å	17.5907(6)
c/Å	20.7908(5)
β/°	91.6972(18)
V/Å^3	4827.8(2)
Z	4
μ/mm^{-1}	0.833
Reflections collected/unique	16005/9484
R_{int}	0.0351
Reflections with $I > 2\sigma(I)$	7030
$R1$ [$I \geq 2\sigma(I)$]	0.0512
$wR2$ [$I \geq (I)$]	0.1293

Table 2 Selected bond lengths (Å) and angles (°) for complex **2**

Mo(1)–C(5)	2.154(4)	Mn(1)–N(1)	2.257(4)
Mo(1)–C(4)	2.156(4)	Mn(1)–N(4)^i	2.270(4)
Mo(1)–C(3)	2.156(5)	Mn(2)–N(6)	2.243(4)
Mo(1)–C(1)	2.158(4)	Mn(2)–O(1W)	2.362(4)
Mo(1)–C(6)	2.165(4)		
Mo(1)–C(8)	2.165(5)		
Mo(1)–C(7)	2.165(5)		
Mo(1)–C(2)	2.170(4)		
Mo1 · · · Mn(1)	5.3619(7)	Mn1 · · · Mn2	7.1824(9)
Mo1 · · · Mn1^{ii}	5.2909(7)	Mn1 · · · Mn2^{iii}	7.8916(10)
Mo1 · · · Mn2	5.4231(7)	Mn1 · · · Mn1^{iv}	8.9034(12)
N(1)–C(1)–Mo(1)	176.6(3)	C(4)–Mo(1)–C(1)	143.33(16)
N(2)–C(2)–Mo(1)	178.2(4)	C(4)–Mo(1)–C(6)	111.25(15)
N(3)–C(3)–Mo(1)	175.9(5)	C(1)–Mo(1)–C(6)	76.72(14)
N(4)–C(4)–Mo(1)	178.0(3)		
N(5)–C(5)–Mo(1)	178.5(4)	N(1)–Mn(1)–N(4)^i	177.57(13)
N(6)–C(6)–Mo(1)	177.6(4)	N(6)–Mn(2)–O(1W)	173.03(16)
N(7)–C(7)–Mo(1)	179.2(5)	N(8)–C(8)–Mo(1)	177.3(4)

Symmetry relations: i 2 − x, ½ + y, ½ − z; ii 2 − x, y − ½, ½ − z; iii x, −y + ½, z − ½; iv 2 − x, 1 − y, −z.

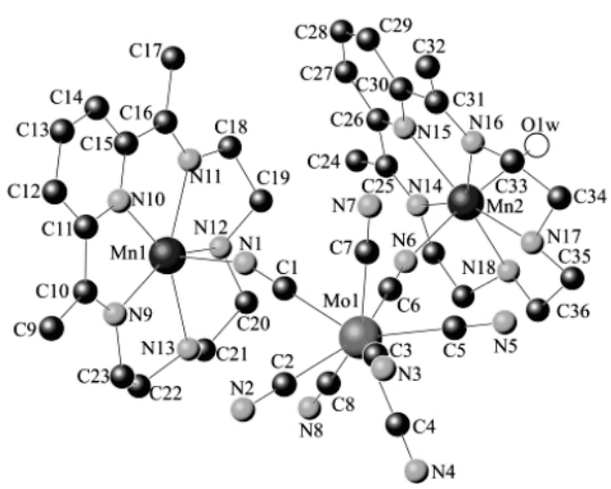

Fig. 2 View of the asymmetric unit for complex **2**. Water molecules are omitted for clarity.

the b direction, a third one is bridging one manganese site (Mn2) and the five remaining cyano groups are terminal (see Fig. 2). The Mo1–C distances are homogenous, ranging from 2.154(4) to 2.170(4) Å with an average distance of 2.161 Å (Table 2). All manganese sites are surrounded by the five nitrogen atoms of the macrocycle in the equatorial plane and co-ordinated by two other atoms along the apical directions, leading to a pentagonal bipyramid geometry. Mn1 is surrounded by seven nitrogen atoms, five from the macrocycle, with Mn1–N distances ranging from 2.262(4) to 2.317(4) Å

Table 3 Selected distances (Å) between CN (non-bonding) and O (non-co-ordinated)

N2 · · · O3w	5.730	N5 · · · O6w^{vii}	5.683
N3 · · · O3w	2.717	N5 · · · O2w^{vi}	5.891
N3 · · · O3w^v	5.549	N7 · · · O2w	2.886
N3 · · · O5w	5.680	N7 · · · O4w	3.002
N3 · · · O2w	5.745	N7 · · · O6w^{viii}	4.855
N5 · · · O6w	2.778	N7 · · · O3w	4.910
N5 · · · O5w	3.536	N7 · · · O5w^{viii}	5.081
N5 · · · O4w^{vi}	4.797		

Symmetry relations: v 1 − x, −y, −z; vi 1 − x, ½ + y, ¾ − z; vii 1 − x, −y, 1 − z; $viii$ 1 − x, ½ + y, ½ − z.

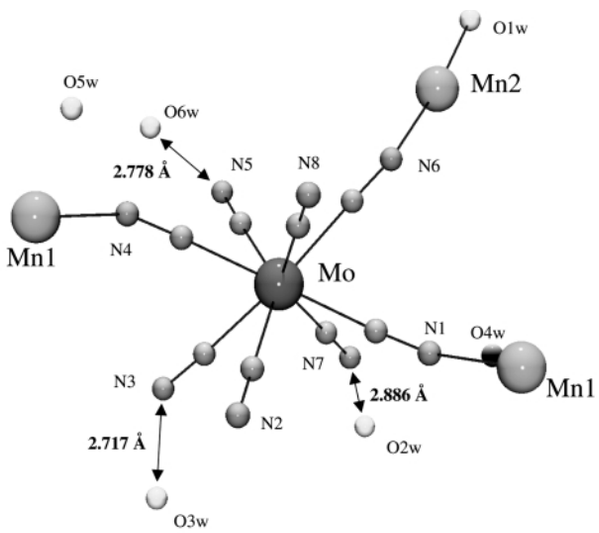

Fig. 3 Detail of the shortest distances between the non-bridging cyano groups and the oxygens of the non-co-ordinated water molecules.

(mean distance 2.293 Å) (Table 2). It is displaced from the mean plane defined by the five nitrogen atoms of the macrocycle by 0.014(2) Å and is bonded to N1–C1–Mo1 (Mn1–N1 2.257(4) Å) and N4–C4–Mo1 (Mn1–N4 2.270(4) Å) linkages along the two apical directions. The Mn2 site is displaced from the plane made of the five nitrogen atoms of the macrocycle by 0.092(2) Å, the distances between Mn2 and nitrogen atoms belonging to the macrocycle are less homogeneous than those from Mn1, ranging from 2.255(4) to 2.303(6) Å with a mean value of 2.286 Å. Mn2 is bonded to the N6–C6–Mo1 linkage along one apical direction and one water molecule along the other apical direction.

The structure contains six water molecules. One molecule is linked to Mn2 (O1W–Mn2 2.362(4) Å). Short contacts exist between some non-bridging cyano groups and four oxygen atoms of non-co-ordinated water molecules (see Table 3 and Fig. 3). These short distances are probably due to the formation of hydrogen bonds but it was impossible to locate the hydrogen atoms. Only atom O5w does not develop short contacts with non-bridging nitrogen atoms, the shortest interaction taking place between O5w and O2w (2.968(7) Å).

Photomagnetic properties of $K_4[Mo^{IV}(CN)_8]\cdot 2H_2O$ 1

In order to understand the photomagnetic properties of compound **2**, we first studied the precursor **1**. Indeed, the existence of photo-oxidation of Mo^{IV} to Mo^{V} under UV-light irradiation in the solid state has to be confirmed. In $K_4[Mo^{IV}(CN)_8]\cdot 2H_2O$ the co-ordination polyhedron around the Mo^{IV} ion is a dodecahedron (D_{2d}) and the polar O–H bonds of the water molecules develop strong interactions with the π-orbital systems of the cyano groups.[40,41]

The magnetisation *versus* field curve of compound **1** before irradiation at 10 K corresponds to a diamagnetic behaviour, as

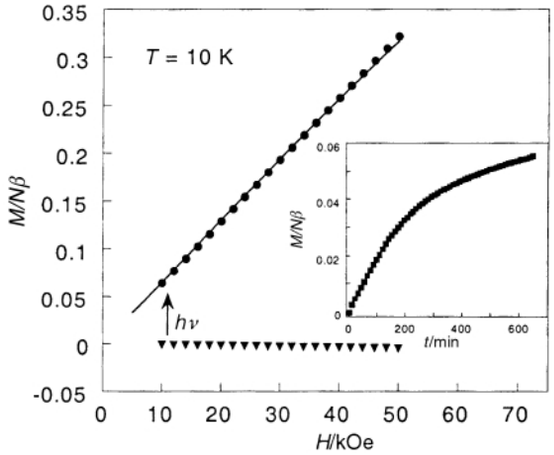

Fig. 4 Field dependence of the magnetisation M at 10 K for $K_4[Mo^{IV}(CN)_8]\cdot 2H_2O$ before (▼) and after (●) UV-light irradiation compared to the Brillouin function for $S = 1/2$ (−). The insert shows the time dependence of the magnetisation upon irradiation.

is expected for Mo^{IV} ($S = 0$). Under UV-light irradiation the magnetisation increased continuously, became positive and gradually reached saturation. The light was switched off after 10 hours of irradiation even if the photo-stationary state, corresponding to a quantitative photochemical yield, was not totally reached (see insert of Fig. 4). The resulting photo-induced magnetisation was observed to be stable, and its field dependence after irradiation at 10 K is in very good agreement with the Brillouin function for a $S = 1/2$ spin state, estimating the conversion to be 98%, as shown in Fig. 4. These observed modifications are not thermally or light reversible.

X-Band Electron Spin Resonance (ESR) experiments were performed at 10 K on the $K_4[Mo^{IV}(CN)_8]\cdot 2H_2O$ powder sample. Before irradiation the compound is ESR silent, as expected for a diamagnetic species. The sample was irradiated in a SQUID cavity and ESR measurements performed just after. The spectrum after irradiation, at 10 K, presents a sharp isotropic signal ($\Delta H_{pp} = 20$ Gauss) centred to a g value close to 2. This is consistent with a paramagnetic compound with $S = 1/2$ and with the photomagnetic properties observed during the SQUID experiment. After one month at room temperature the compound presents an identical ESR signal at low temperature, confirming a thermally non-reversible effect.

The change from a diamagnetic to a paramagnetic state under UV-light irradiation can be explained by a photo-oxidation of the diamagnetic Mo^{IV} to the paramagnetic Mo^{V} possessing a spin $S = 1/2$. The molybdenum oxidation is accompanied by a reduction of one water molecule of the lattice and we propose the mechanism in eqns. (1) and (2). The

$$K_4[Mo^{IV}(CN)_8]\cdot 2H_2O \xrightarrow{h\nu} K_4[Mo^{IV}(CN)_8]^*\cdot 2H_2O \quad (1)$$

$$K_4[Mo^{IV}(CN)_8]^*\cdot 2H_2O \longrightarrow K_3[Mo^{V}(CN)_8]\cdot H_2O + (K^+,OH^-) + \tfrac{1}{2}H_2(g) \quad (2)$$

existence of this internal photochemical redox reaction under UV-light irradiation is directly related to the presence of $[Mo^{IV}(CN)_8]^{4-}$ in an excited state which is a much better reductant than in its ground state. The vicinity of the water molecules to the cyanide ligands is another key factor for the electron transfer. Even if not observed, the release of hydrogen gas from the structure may explain the thermal non-reversibility of the photo-induced magnetic properties. This behaviour in the solid state is analogous to the photochemical properties in solution of the $[Mo^{IV}(CN)_8]^{4-}$ ion irradiated in charge transfer bands.[13–17]

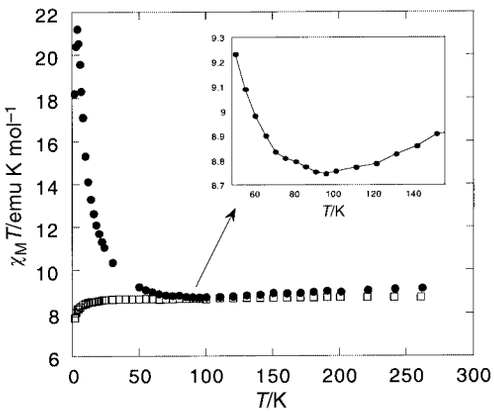

Fig. 5 $\chi_m T$ *versus* T plot before (□) and after (●) irradiation for complex **2** under a magnetic field of 1 kOe. The insert shows the detail of the minimum in the $\chi_m T$ curve.

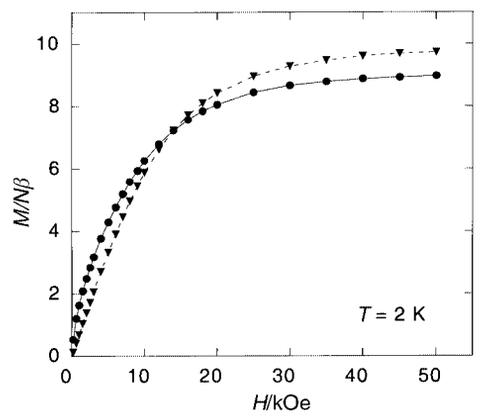

Fig. 6 Field dependence of the magnetisation M at 2 K for complex **2** before (▼) and after (●) irradiation.

Interesting photomagnetic effects are thus expected for extended polymetallic systems due to the intrinsic properties of Mo^{IV} under UV-light irradiation.

Magnetic and photomagnetic properties of $[Mn^{II}_2(L)_2(H_2O)][Mo^{IV}(CN)_8]\cdot 5H_2O$ 2

The temperature dependence of the $\chi_m T$ product in the range 2–300 K for compound **2** is shown in Fig. 5. The $\chi_m T$ value at room temperature before irradiation, 8.74 cm^3 K mol^{-1}, is what is expected for two uncoupled high spin Mn^{II} ($S = 5/2$) assuming $g = 2$. As the temperature is lowered $\chi_m T$ is constant and slowly decreases at low temperature indicating the presence of weak antiferromagnetic interactions. Since the shortest through-space distance between manganese ions is larger than 9 Å, these antiferromagnetic interactions probably take place between Mn^{II} through the NC–Mo^{IV}–CN diamagnetic bridges (see Table 2). This behaviour is similar to what has been observed in the three-dimensional compounds synthesized with $[Mo^{IV}(CN)_8]^{4-}$.[26] The magnetisation M *versus* field curve recorded at 2 K for **2** is below the Brillouin function curve and reaches at 50 kOe a value of 9.75 $N\beta$ (N is the Avogadro number, β is the Bohr magneton) as expected for weak antiferromagnetic interactions between two Mn^{II} (see Fig. 6).

Under UV-light irradiation at 10 K the magnetisation of compound **2** at 1 kOe increased rapidly and then slowly reached saturation. The light was turned off after 10 hours of irradiation and the photo-induced magnetisation was observed to be stable. Then, all magnetic data were recorded without light irradiation.

The field dependence of magnetisation at 2 K after irradiation is shown in Fig. 6. The curve reaches saturation at 8.96 $N\beta$ with an external field of 50 kOe, as expected for a system of two spins $S = 5/2$ and one spin $S = 1/2$ with antiferromagnetic inter-

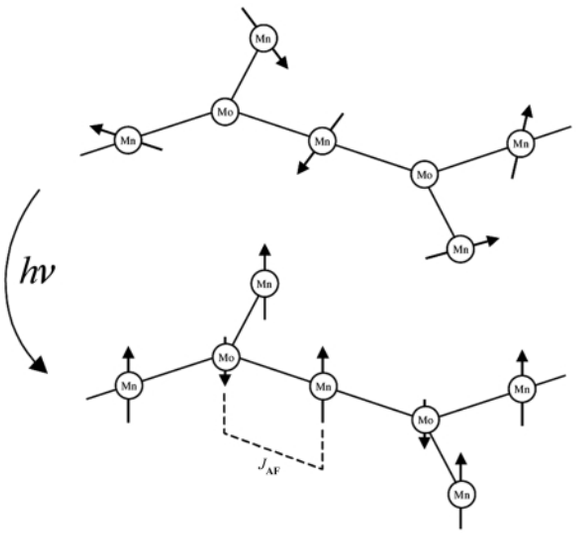

Fig. 7 Scheme of the intra-chain antiferromagnetic interactions, photo-induced under UV-light irradiation, between Mo and Mn.

actions. The $\chi_m T$ *versus* T curve was recorded in warming mode in the range 2–260 K under a magnetic field of 1 kOe. The result is shown Fig. 5. At very low temperature the curve increases, when the temperature is increased, reaches a maximum of 21.2 cm^3 K mol^{-1} at 4 K, then rapidly decreases until a shallow minimum of 8.74 cm^3 K mol^{-1} at ≈95 K. From 100 K, $\chi_m T$ continuously increases when the temperature is increased further. The $\chi_m T$ value observed at 260 K is 9.14 cm^3 K mol^{-1}, close to the value (9.125 cm^3 K mol^{-1}) expected for non-interacting two $S_{Mn} = 5/2$ and one $S_{Mo} = 1/2$ spins. The modifications of magnetic properties observed at 10 K are maintained after thermal treatment at room temperature, showing the irreversibility of the phenomenon.

The magnetic behaviour of compound **2** after irradiation is consistent with the formation of ferrimagnetic chains with a characteristic minimum in the $\chi_m T$ *versus* T plot.[42] The observed increase of the magnetisation at low field clearly indicates the increase of the spin correlation length within the chain. The antiferromagnetic intra-chain interactions between the metal ions (Mn^{II} and Mo^{V}) are consistent with the saturation value of ≈9 $N\beta$ for magnetisation at 2 K (see Fig. 6). The decrease of the $\chi_m T$ plot below 4 K is probably due to inter-chain antiferromagnetic interactions, the shortest distance being 7.016 Å between the Mn2 and Mo1 sites of two different chains along the c direction (see Fig. 1). The spin topology of the photo-generated chain is rather complicated; it corresponds to an alternated spin chain ($S_{Mo1} = 1/2$ and $S_{Mn1} = 5/2$) with a pendant arm ($S_{Mn2} = 5/2$). To the best of our knowledge, no theoretical model exists for this spin topology. It is therefore impossible with our data to estimate the exchange parameter J_{AF} between the metal ions. However, the minimum in the $\chi_m T$ *versus* T curve at 95 K allows us to think that these intra-chain antiferromagnetic interactions are rather strong for molecular compounds.[11,12,42]

As in the case of the $K_4[Mo^{IV}(CN)_8]\cdot 2H_2O$ precursor, the mechanism involved in the change of magnetic properties is a photo-oxidation of Mo^{IV} to Mo^{V} under UV-light irradiation. Indeed, the crystallographic data give us precise information about the structure of the chain and the geometry around the Mo^{IV}. On the one hand, of the eight cyanide ligands around the molybdenum, five remain non-bridging and three are linked to a $Mn^{II}(L)$ unit. On the other hand, some non-co-ordinated water molecules probably develop hydrogen bonds with the nitrogens of the non-bridging cyanide ligands in the light of the short contacts found in the structure (see Table 3). This arrangement around the Mo^{IV} in compound **2** is similar to the one observed in the precursor. The photo-oxidation process occurring in the precursor under UV-light irradiation is then operative in compound **2**.

Before irradiation, the magnetisation *versus* field and the temperature dependence of the $\chi_m T$ product indicate that the system is paramagnetic with two uncoupled Mn^{II} per formula unit. Upon irradiation, the Mo^{IV} is photo-oxidised to Mo^{V} by ejection of an electron. This photo-oxidation, due to the presence of non-bridging cyanide ligands close to water molecules, generates new magnetic interactions between adjacent Mn^{II} and Mo^{V}. In time, the correlation length increases and the system becomes equivalent to a ferrimagnetic chain with a topology as represented in Fig. 7. As in the case of the precursor, the photo-oxidation is a thermally non-reversible phenomenon leading to permanent magnetic modifications of compound **2**.

Conclusion

A new one-dimensional bimetallic chain has been obtained by reaction between $K_4[Mo^{IV}(CN)_8]\cdot 2H_2O$ and a $Mn^{II}(L)$ complex (L = macrocycle) with two-available co-ordination sites; its crystal structure has been solved. The compound, formulated as $[Mn^{II}_2(L)_2(H_2O)][Mo^{IV}(CN)_8]\cdot 5H_2O$ **2**, has a zigzag chain structure of alternative Mn^{II} and Mo^{IV} with another Mn^{II} linked to the Mo^{IV} as a pendant arm. Under UV-light irradiation, the diamagnetic Mo^{IV} is photo-oxidised to paramagnetic Mo^{V} generating new antiferromagnetic interactions between the metal ions. This photo-generation of magnetic centers induces the formation of ferrimagnetic chains of Mn^{II} ($S_{Mn} = 5/2$) and Mo^{V} ($S_{Mo} = 1/2$). This change of magnetic properties is not reversible, even after thermal treatment at room temperature. The particular behaviour of **2** is due to the intrinsic property of $K_4[Mo^{IV}(CN)_8]\cdot 2H_2O$ which presents a photo-oxidation of Mo^{IV} to Mo^{V} under UV-light irradiation. This work has confirmed that this property is conserved even in the solid state.

The property of the octacyanomolybdate precursor has also been observed for the $K_4[W^{IV}(CN)_8]\cdot 2H_2O$ complex. Interesting photomagnetic effects are thus expected for polymetallic systems synthesized with these octacyanometalate complexes. Furthermore, a great variety of structures are conceivable with these building blocks due to their flexible geometry (dodecahedral, square antiprism …) combined with the transition metal ions.[43] We hope to report in the very near future some reversible photomagnetic effects on finite (0-D) and extended (3–D) compounds.

Acknowledgements

This work is partly funded by the TMR Research Network ERBFMRXCT980181 of the European Union, entitled "Molecular Magnetism; from Materials towards Devices".

References

1 O. Sato, T. Iyoda, A. Fujishima and K. Hashimoto, *Science*, 1996, **272**, 704.
2 M. Verdaguer, *Science*, 1996, **272**, 698.
3 Z.-Z. Gu, O. Sato, T. Iyoda, K. Hashimoto and A. Fujishima, *J. Phys. Chem.*, 1996, **100**, 18289.
4 O. Sato, Y. Einaga, A. Fujishima and K. Hashimoto, *Inorg. Chem.*, 1999, **38**, 4405.
5 S. Ohkoshi and K. Hashimoto, *J. Am. Chem. Soc.*, 1999, **121**, 10591.
6 K. Yoshizawa, F. Mohri, G. Nuspl and T. Yamabe, *J. Phys. Chem. B*, 1998, **102**, 5432.
7 A. Goujon, O. Roubeau, F. Varret, A. Dolbecq, A. Bleuzen and M. Verdaguer, *Eur. Phys. J. B*, 2000, **14**, 115.
8 S. Decurtins, P. Gütlich, C. P. Köhler, H. Spiering and A. Hauser, *Chem. Phys. Lett.*, 1984, **105**, 1; A. Hauser, *Chem. Phys. Lett.*, 1986, **124**, 543.
9 A. Hauser, *Coord. Chem. Rev.*, 1991, **111**, 275.
10 J. F. Létard, L. Capes, G. Chastanet, N. Moliner, S. Létard, J. A. Real and O. Kahn, *Chem. Phys. Lett.*, 1999, **313**, 115.
11 Y. Sano, M. Tanaka, N. Koga, K. Matsuda, H. Iwamura, P. Rabu and M. Drillon, *J. Am. Chem. Soc.*, 1997, **119**, 8246.

12 S. Karasawa, Y. Sano, T. Akita, N. Koga, T. Itoh, H. Iwamura, P. Rabu and M. Drillon, *J. Am. Chem. Soc.*, 1998, **120**, 10080.
13 W. L. Waltz and A. W. Adamson, *J. Phys. Chem.*, 1969, **73**, 4250.
14 W. L. Waltz, A. W. Adamson and P. D. Fleischauer, *J. Am. Chem. Soc.*, 1967, **89**, 3923.
15 M. Shirom and Y. Siderer, *J. Chem. Phys.*, 1972, **57**, 1013.
16 M. Shirom and Y. Siderer, *J. Chem. Phys.*, 1973, **58**, 1250.
17 A. Vogler, W. Losse and H. Kunkely, *J. Chem. Soc.*, *Chem. Commun.*, 1979, 187.
18 A. Bettelheim and M. Shirom, *Chem. Phys. Lett.*, 1971, **9**, 166.
19 R. P. Mitra, B. K. Sharma and H. Mohan, *Aust. J. Chem.*, 1972, **25**, 499.
20 R. L. Marks and E. Popielski, *Inorg. Nucl. Chem. Lett.*, 1974, **10**, 885.
21 V. Balzani, M. F. Manfrin and L. Moggi, *Inorg. Chem.*, 1969, **8**, 47.
22 R. D. Archer and D. A. Drum, *J. Inorg. Nucl. Chem.*, 1974, **36**, 1979.
23 F. McKnight and G. P. Haight, *Inorg. Chem.*, 1973, **12**, 3007.
24 A. K. Sra, G. Rombaut, F. Lahitête, S. Golhen, L. Ouahab, J. V. Yakhmi, C. Mathonière and O. Kahn, *New J. Chem.*, submitted.
25 H. Hennig, A. Rehorek, D. Rehorek and Ph. Thomas, *Inorg. Chim. Acta*, 1984, **86**, 41.
26 G. Rombaut, M. Verelst, C. Mathonière and O. Kahn, unpublished work.
27 J. L. Heinrich, P. A. Berseth and J. R. Long, *Chem. Commun.*, 1998, 1231.
28 S. Zhan, X. Chen, A. Vij, D. Guo and Q. Meng, *Inorg. Chim. Acta*, 1999, **292**, 157.
29 K. Van Langeberg, S. R. Batten, K. J. Berry, D. C. R. Hockless, B. Moubaraki and K. Murray, *Inorg. Chem.*, 1997, **36**, 5006.
30 M. Ohba, N. Maruono, H. Okawa, T. Enoki and J. M. Latour, *J. Am. Chem. Soc.*, 1994, **116**, 11566.
31 M. Ohba, H. Okawa, N. Fukita and Y. Hashimoto, *J. Am. Chem. Soc.*, 1997, **119**, 1011.
32 M. S. El Fallah, E. Rentschler, A. Caneschi, R. Sessoli and D. Gatteschi, *Angew. Chem.*, *Int. Ed. Engl.*, 1996, **35**, 1947.
33 S. Tanase, G. Rombaut, C. Mathonière, T. Maris, D. Chasseau, M. Andruh and O. Kahn, unpublished work.
34 A. K. Sra, M. Andruh, O. Kahn, S. Golhen, L. Ouahab and J. V. Yakhmi, *Angew. Chem.*, *Int. Ed.*, 1999, **38**, 2606.
35 J. G. Leipoldt, L. D. C. Bok and P. J. Cilliers, *Z. Anorg. Allg. Chem.*, 1974, **409**, 343.
36 O. Jiménez-Sandoval, D. Ramirez-Rosales, M. J. Rosales-Hoz, M. E. Sosa-Torres and R. Zamorano-Ulloa, *J. Chem. Soc.*, *Dalton Trans.*, 1998, 1551.
37 Z. Otwinowski and W. Minor, *Processing of X-Ray Diffraction Data Collected in Oscillation Mode*, Academic Press, New York, 1996.
38 G. M. Sheldrick, SHELX 97, Program for the Refinement of Crystal Structures, University of Göttingen, 1997.
39 J. R. Perumareddi, A. D. Liehr and A. W. Adamson, *J. Am. Chem. Soc.*, 1963, **85**, 249.
40 J. L. Hoard, T. A. Hamor and M. D. Glick, *J. Am. Chem. Soc.*, 1968, **90**, 3177.
41 E. L. Muetterties, *Inorg. Chem.*, 1973, **12**, 1963.
42 O. Kahn, Y. Pei, M. Verdaguer, J. P. Renard and J. Sletten, *J. Am. Chem. Soc.*, 1988, **110**, 782.
43 Z. J. Zhong, H. Seino, Y. Mizobe, M. Hidai, A. Fujishima, S. Ohkoshi and K. Hashimoto, *J. Am. Chem. Soc.*, 2000, **122**, 2952.